Coupled Atomistic and Discrete Dislocation Plasticity

L. E. Shilkrot,[1] R. E. Miller,[2] and W. A. Curtin[1]

[1]*Division of Engineering, Brown University, Providence, Rhode Island 02912*
[2]*Department of Mechanical and Aerospace Engineering, Carleton University, Ottawa, Ontario, Canada, K1S 5B6*

A computational method for multiscale modeling of plasticity is presented wherein each dislocation is treated as either an atomistic or continuum entity within a single computational framework. The method divides space into atomistic and continuum regions that communicate across a coherent boundary, detects dislocations as they approach the boundary, and seamlessly converts them from one description to another. The method permits the study of problems that are too large for fully atomistic simulation while preserving accurate atomistic details where necessary, but is currently limited to a 2D implementation. A validation test is performed by comparing the method against full atomistic simulations for a 2D nano-indentation problem.

Plastic deformation and fracture of ductile materials involves important physical phenomena at multiple length scales. Some phenomena (e.g., dislocation nucleation, mobility, cross-slip, crack formation, and growth) are intrinsically atomistic. Atomistic studies can address these "unit" processes involving a few defects but are usually unable to address larger-scale deformation except with supercomputers. Plastic deformation at the micron scale, due to motion and interaction of many dislocations, can be described by representing the dislocations as continuum line defects and neglecting the dislocation core structure [1−3]. Such continuum models include atomistic effects only through phenomenological rules. Some atomistic effects, such as dislocation mobility and cross-slip, are amenable to phenomenological description while others, such as dislocation nucleation and crack growth, may defy description by simple rules. A true coupled multiscale model should be capable of dealing with the necessary atomistic degrees of freedom simultaneously with the continuum degrees of freedom, including all long-range interactions, within one overall computational scheme. In this Letter we describe such a method: the coupled atomistic and discrete dislocation (CADD) method.

CADD consists of a fully atomistic region, with arbitrary complexity, directly coupled to a linear elastic continuum region containing dislocations modeled as continuum elastic line defects. CADD thus minimizes the number of atoms required to include atomic-scale phenomena and replaces atomic degrees of freedom by continuum degrees of freedom describing the continuum elastic displacements and the dislocation lines with little or no loss of accuracy relative to full atomistics.

A number of multiscale methods (e.g., [4−8]), connect an atomistic region to a defect-free continuum region. Key and distinguishing features of CADD are that (i) dislocations exist in the continuum region, (ii) they are mechanically coupled to one another and to the atomistic region, and (iii) they can be passed between the atomistic and continuum regions so that the plastic deformation is not confined to the atomistic region. Passing of dislocations requires two main developments described below: (i) detection of dislocations near the atomic/continuum interface that are candidates for passing and (ii) a procedure for moving such dislocations across the interface. The passing methodology here restricts the current CADD method to 2D problems; extension to 3D is discussed below. As a test of the current model, we compare its predictions against full atomistic simulations for a 2D nano-indentation problem and find good agreement.

Mechanics deals with the solution of boundary value problems (b.v.p.). The general b.v.p. solved here is shown schematically in Fig 1. A body is divided into one or more atomistic regions Ω_A and one or more linear elastic, continuum regions Ω_C. Interfaces $\partial\Omega_I$ are between atomistic and continuum regions. Tractions $\boldsymbol{T} = \boldsymbol{T}_0$ are prescribed on $\partial\Omega_T$ and displacements $\boldsymbol{u} = \boldsymbol{u}_0$ on $\partial\Omega_u$. Region Ω_C contains N continuum discrete dislocations with Burgers vectors $\boldsymbol{b}^i$ and positions $\boldsymbol{d}^i$ ($i = 1 \ldots N$). In the atomistic regions, any atomic scale defects (dislocations, grain boundaries, vacancies, voids, amorphous regions) may exist. The only assumption about these atomistic regions is that near the interfaces with the continua their behavior approaches the linear elastic continuum response. The solution to this b.v.p., consisting of atom positions $\boldsymbol{r}_A$, dislocation positions $\boldsymbol{d}^i$ and continuum displacements $\boldsymbol{u}$, stresses $\boldsymbol{\sigma}$, and strains $\boldsymbol{\epsilon}$, is obtained by considering separate problems in the continuum (in Fig. 1, Problems I and II) and atomistic (in Fig. 1, Problem III) domains, generated by cutting the system along the interface $\partial\Omega_I$ while enforcing continuity of displacements across $\partial\Omega_I$.

The fields in the continuum region can be treated using the standard discrete dislocation (DD) method [1]. Specifically, the continuum problem is divided into two complementary problems (Fig. 1). Problem I consists of dislocations in an infinite elastic continuum and is solved by superposition of the analytical elastic fields due to the
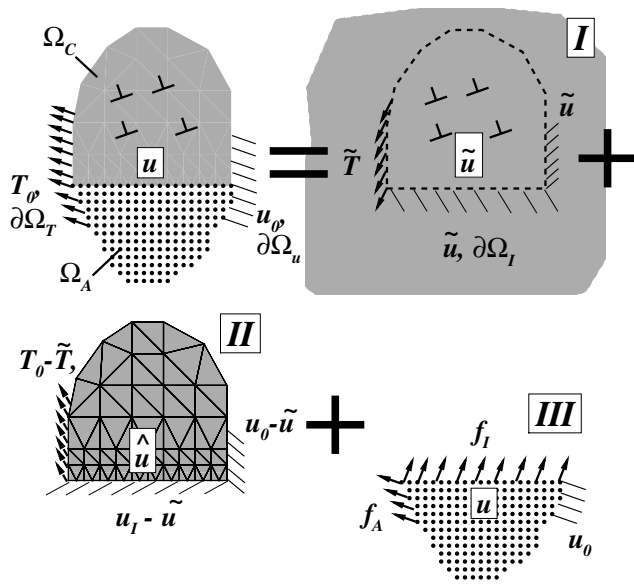
FIG. 1. Schematic illustration of the CADD solution procedure.

individual dislocations at positions d^i. We denote the total field as the ˜ field. Problem I generates tractions $\tilde{T}$ along $\partial\Omega_T$ and displacements $\tilde{u}$ and $\tilde{u}_I$ along $\partial\Omega_u$ and $\partial\Omega_I$ that differ from the prescribed values of T_0, u_0, and the u_I imposed by the atomistic region. Problem II is designed such that, when superimposed with Problem I, the desired boundary conditions imposed on the continuum problem are satisfied exactly. Problem II thus consists of a linear elastic continuum with no dislocations but subject to "corrective" tractions $\hat{T} = T_0 - \tilde{T}$ on $\partial\Omega_T$ and "corrective" displacements $\hat{u} = u_0 - \tilde{u}$ on $\partial\Omega_u$ and $\hat{u} = u_I - \tilde{u}_I$ on $\partial\Omega_I$. All discontinuities and singularities of the dislocations are contained in the ˜ fields of Problem I, so the fields of Problem II, denoted as ˆ fields, are smooth and obtainable numerically. The total fields in the continuum are the superpositions of the fields from Problems I and II: $u = \tilde{u} + \hat{u}$, $\sigma = \tilde{\sigma} + \hat{\sigma}$, and $\epsilon = \tilde{\epsilon} + \hat{\epsilon}$.

Problem III in Fig. 1 deals with the atomistic region. Away from the interface it is treated in a standard manner using interatomic potentials as functions of the atom positions r_A. The subtlety in any atomistic/continuum method lies in treatment of the interface. Numerous approaches exist to connect a strictly *local* continuum region to an inherently *nonlocal* atomistic region (due to the range r_{cut} of the potentials); e.g., [4–8]. Abruptly cutting the model along an atomic plane as in Fig. 1 introduces spurious surface energy and relaxation at the interface. To minimize such errors, we introduce a pad of atoms (positions r_P) of thickness r_{cut} outside of the defined atomistic region and overlapping the continuum region, as shown in Fig. 2(a), with a free outer surface. With such a pad, the atoms r_A behave more like proper "bulk" atoms. The pad of atoms introduces extra energy by double counting the overlapped

material and makes the region artificially stiff against deformation parallel to the interface, but mitigates the major problems associated with a sharp interface cut. Other interfacing schemes could be employed here but neither the detecting nor passing of dislocations in CADD are affected by the method for handling the interface.

With the above decomposition of the desired b.v.p., the energy functional for the entire system can be expressed as

$$\Psi = \frac{1}{2}\int_{\Omega_C}(\tilde{\sigma} + \hat{\sigma}):(\tilde{\epsilon} + \hat{\epsilon})dV$$
$$- \int_{\partial\Omega_C}T_0 \cdot u \, dA + E_{at}(r_A, r_I, r_P) - f_A \cdot u_A,$$

where E_{at} is the atomistic energy, subscripts A, I, and P distinguish bulk, interface, and pad atoms, respectively, u_A denotes atom displacements, and f_A denotes the applied tractions T_0 resolved into forces on individual atoms along $\partial\Omega_T$.

We then discretize the ˆ fields (Problem II) using a standard finite element mesh with nodal displacements $\hat{u}_C$ in Ω_C and $\hat{u}_I$ along $\partial\Omega_I$, where nodes correspond exactly to atoms. The interface atom-node pairs are forced to have the same displacements throughout the deformation to ensure compatibility. Fully anisotropic linear elastic finite elements are used to match the crystalline elastic constants. The ˜ fields (Problem I) use dislocation fields based on isotropic elasticity, introducing a small error. After discretizing and using the reciprocal theorem, the energy functional becomes

$$\Psi = \frac{1}{2}\int_{\Omega_C}\tilde{\sigma}:\tilde{\epsilon}dV$$
$$+ \frac{1}{2}(\hat{u}_C \cdot C_{CC} \cdot \hat{u}_C + \hat{u}_I \cdot C_{II} \cdot \hat{u}_I)$$
$$+ \hat{u}_C \cdot C_{CI} \cdot \hat{u}_I + \tilde{t}_I \cdot \hat{u}_I - \tilde{t}_C \cdot \hat{u}_C - \hat{t}_0 \cdot \tilde{u}_C$$
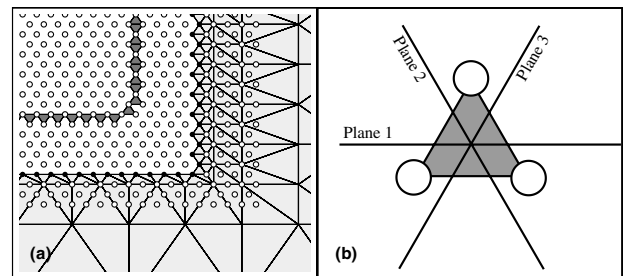$$+ E_{at}(r_A, r_I, r_P) - f_A \cdot u_A,$$

FIG. 2. (a) Closeup of the atomistic/continuum interface. Continuum elements are light gray. The sharp interface of atoms/nodes is shown by filled circles; unfilled circles in the continuum region constitute the "pad" of atoms to mitigate surface effects; other unfilled circles show atoms in the atomistic region. The dark gray elements are the dislocation "detection band." (b) A closeup of one detection element, indicating the three slip planes passing through it.

where C_{CC}, C_{II}, C_{CI} represent the FEM stiffness matrices coupling the various continuum displacements and $\hat{t}_C, \tilde{t}_I$, and t_0 are resolved nodal forces. The remaining integral is the elastic energy in Ω_C of the infinite-space dislocations and requires special care due to the singularities in the dislocation fields. We use the Airy stress function χ to represent the analytic dislocation stress field $\tilde{\sigma}$, which permits the dislocation energy to be expressed as a sum of direct dislocation interactions and a single integral over the continuum boundary $\partial\Omega = \partial\Omega_C + \partial\Omega_I$ given by

$$\int_{\Omega_C} \tilde{\sigma} : \tilde{\epsilon}\, dV = \sum_{i=1...N} \left[\frac{\partial\chi_i'(d^i)}{\partial y} b_x^i - \frac{\partial\chi_i'(d^i)}{\partial x} b_y^i \right] - 2\int_{\partial\Omega}\left[\left(\frac{\partial\chi}{\partial y}\right)\nabla u_x - \left(\frac{\partial\chi}{\partial x}\right)\nabla u_y \right] d\gamma \,,$$

where $\chi_i'(d^i)$ is the stress function for all but the ith dislocation evaluated at d^i.

Since Problem II is linearly elastic, minimization of the energy with respect to the continuum nodal degrees of freedom can be performed, leading to additional forces f_I on the interface atoms (corresponding to the nodes u_I). The conjugate gradient (CG) technique is then used to minimize the reduced energy functional and move *both* the atoms and continuum dislocations to their equilibrium positions. As a natural consequence, the total force (from interatomic potentials and nodal forces f_I) on the interfacial atoms vanishes at the equilibrium.

In the atomistic regions, dislocations will nucleate during the energy minimization. Such dislocations that move toward the continuum region must be detected and "passed" to the continuum region. We define a "detection band" of triangular elements between atoms inside Ω_A with each element sitting on three different slip planes, as shown in Fig. 2. If a dislocation passes along one of these planes, it generates a Lagrangian finite strain in the element of

$$E = \frac{(b^i \otimes m)_{\text{sym}}}{d} + \frac{(m \otimes b^i)(b^i \otimes m)}{2d^2} \,,$$

where sym implies the symmetric part of a matrix, m is the slip plane normal, d is the interplanar spacing, and $\otimes$ is the tensor product. For a given crystal structure and orientation, all the possible slip systems and associated strains E are known. The detection algorithm monitors the strains in the detection band elements and compares them to the known dislocation slip strains after each CG energy minimization step. When the strain in an element corresponds to a particular dislocation, the dislocation core is assumed to reside at the centroid of that element. Use of the Lagrangian finite strain tensor is essential because the crystal can undergo large deformations involving lattice rotations. Because multiple dislocations can pass through one element, it is necessary to keep track of all previous slip activity and consider only the displacements due to new defects.

Once a dislocation has been identified in an element of the detection band, it must be "passed" to the continuum as a discrete dislocation. The detection establishes the location of the core, the slip plane, and the Burgers vector of the continuum entity. The passing requires careful treatment of the kinematics to maintain continuity across the interface. First, the core is artificially shifted along its slip plane from its location in the detection band to a location across the interface in the continuum region by adding the displacement fields associated with a dislocation dipole. These displacements cancel the original core in the atomistic region and add a new core in the continuum region. Once this core is in the continuum region, it is added to the array of discrete dislocations with care being taken to define the branch cut in the continuum displacement field such that it matches the slip plane along which the dislocation moves. Subsequent relaxation of the atoms naturally anneals out the remnants of the atomic core and moves the dislocation to its continuum equilibrium position.

As a test of the accuracy of the CADD model, we consider a 2D indentation problem on a system size amenable to full atomistic simulations. The problem consists of a rectangular slab, 713 Å high and 466 Å wide (100 701 atoms), of single crystal Al oriented such that the sides are (111) planes and the top and bottom are $(1\bar{1}0)$ planes. The Al is described using EAM potentials and their associated elastic constants. In CADD, the atomistic region is confined to a small region near the corner of the indenter containing 2811 atoms. After constructing a suitable FEM mesh the total number of atoms and nodes is only 3350. The displacements of the atoms along the rigid indenter spanning the left half of the top surface are increased in increments of 0.2 Å and the bottom boundary of the sample is held fixed. The mesh used for the CADD simulation is shown in Fig. 3(a), in its final deformed configuration after the indenter has moved 17 Å. The displacements shown are the total solution $u = \hat{u} + \tilde{u}$.

The simulations are performed until a total of three full dislocations have been nucleated, each of which consist of a pair of closely spaced Shockley partials. Figure 3(b) shows a comparison of the load-displacement curves for the fully atomistic and CADD simulations. Figure 3(c) shows the dislocations positions from initial nucleation at the top of the model (depth = 0) to the equilibrium positions as the penetration of the indenter increases. Note that the bottom of the indenter, at $y = -713$ Å, is a rigid boundary so the dislocations pile up against it. Overall, the agreement is quite good.

Figure 3(b) shows that the CADD dislocations nucleate at the same load step or just one step later than in the full atomistics. The CADD dislocations move further down and there are slight differences in the load-displacement
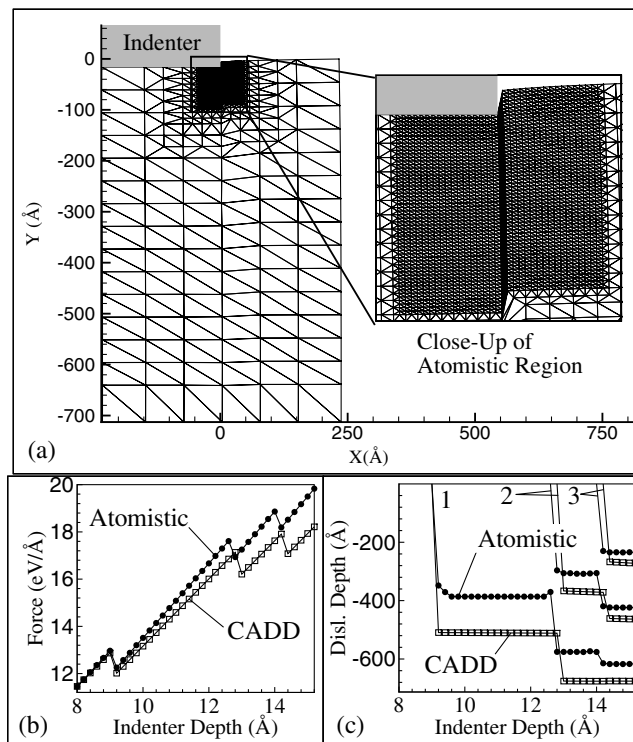
FIG. 3. (a) CADD mesh used to simulate nanoindentation. A deformed finite element mesh is used in the atomistic regime and shows where slip has occurred. (b) Applied load and (c) positions of first three emitted dislocations (labeled 1, 2, and 3) as a function of indenter displacement. Open squares: CADD results. Filled circles: full atomistics.

curves. These effects are all coupled and are likely due to several minor approximations in CADD. The assumption of linear elasticity in the continuum region makes CADD less stiff in compression than the full nonlinear atomistic model, and spurious residual forces at the CADD interface remain and can influence the dislocation motion. Most of these effects can be minimized by using (i) nonlinear FEM in the continuum and/or (ii) a better interface coupling method. An alternative CADD-like method by the present authors that is more precise but also much more cumbersome eliminates some of the small deviations found here [9].

In summary, we have presented a technique that couples a fully atomistic region to a linear elastic region containing discrete dislocations. This is a true multiscale model in that dislocations are treated either fully atomistically or as continuum entities depending on where they are located in space, all within a single framework. Previous efforts treated the continuum region as defect free or neglected

atomistics altogether. Other key strengths of the present model are the automatic detection and passing of dislocations that are nucleated in the atomistic region and move into the continuum region.

The CADD method is currently a 2D equilibrium implementation. In this form, it can provide qualitative understanding of the role of large numbers of dislocations in processes such as grain boundary sliding, atomic scale void growth, and fracture that cannot be easily treated by either fully atomistic models or existing discrete dislocation approaches. When no defects are passed between the atomistic and continuum region, the CADD methodology applies to fully 3D problems. A full 3D formulation for the dislocation passing is quite difficult due to the need for an accurate treatment of dislocation loops that intersect the atomistic/continuum interface. Recent progress [10] on the intersection of continuum dislocation loops with free surfaces may provide some guidance. Other 2D applications and extensions to 3D and to dynamics will be the subject of future work, with the latter expected to be guided by other dynamic hybrid models (e.g., [6]).

[1] E. van der Giessen and A. Needleman, Model. Simul. Mater. Sci. Eng. **3**, 689 (1995).
[2] H. Zbib, M. Rhee, and J. Hirth, Int. J. Mech. Sci. **40**, 113 (1998).
[3] L. Kubin and G. Canova, Scr. Metall. **27**, 957 (1992).
[4] V. B. Shenoy, R. Miller, E. B. Tadmor, R. Phillips, and M. Ortiz, Phys. Rev. Lett. **80**, 742 (1998).
[5] F. F. Abraham, J. Q. Broughton, N. Bernstein, and E. Kaxiras, Comput. Phys. **12**, 538 (1998).
[6] R. E. Rudd and J. Q. Broughton, Phys. Status Solidi B **217**, 251 (2000).
[7] S. Kohlhoff, P. Gumbsch, and H. F. Fischmeister, Philos. Mag. A **64**, 851 (1991).
[8] V. B. Shenoy, R. Miller, E. B. Tadmor, D. Rodney, R. Phillips, and M. Ortiz, J. Mech. Phys. Solids **47**, 611 (1998).
[9] L. E. Shilkrot, W. A. Curtin, and R. E. Miller, J. Mech. Phys. Solids (to be published).
[10] D. Weygand, L. Friedman, E. van der Giessen, and A. Needleman, Model. Simul. Mater. Sci. Eng. (to be published).